

Supplement of Earth Syst. Sci. Data, 12, 1973–1983, 2020  
<https://doi.org/10.5194/essd-12-1973-2020-supplement>  
© Author(s) 2020. This work is distributed under  
the Creative Commons Attribution 4.0 License.



*Supplement of*

## **A deep learning reconstruction of mass balance series for all glaciers in the French Alps: 1967–2015**

**Jordi Bolibar et al.**

*Correspondence to:* Jordi Bolibar ([jordi.bolibar@univ-grenoble-alpes.fr](mailto:jordi.bolibar@univ-grenoble-alpes.fr))

The copyright of individual parts of the supplement might differ from the CC BY 4.0 License.

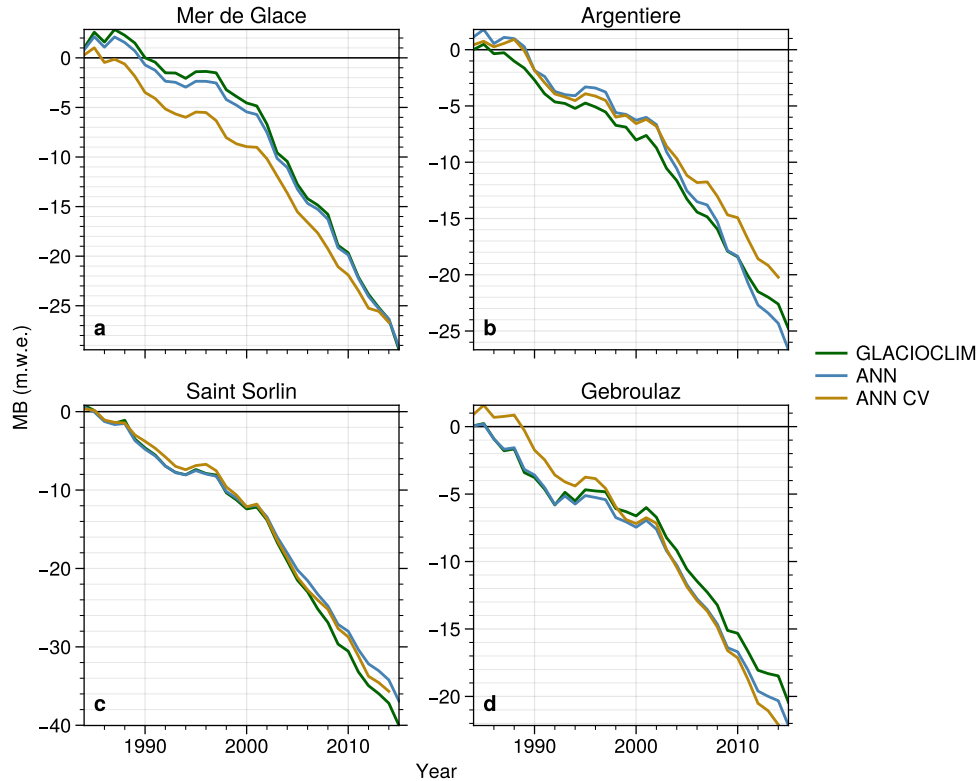


**Figure S1.** Comparison between glaciological observations from the GLACIOCLIM observatory, cross-validated MB reconstructions from this study (ANN CV) and fitted MB reconstructions (ANN). The cross-validated models are shown to display the out-of-sample performance. The fitted reconstructions display the actual reconstructions from the dataset, with models especially fitted for glaciers with data.

## 1 Comparison with independent geodetic mass balance data

All available annual glacier-wide MB data in the French Alps have been used to train the MB ANN of the present study. However, some multi-annual geodetic mass balance (MB) datasets exist that can provide a means to validate the reconstruction's bias for specific glaciers during multi-annual time intervals. This type of analysis is more limited than the cross-validation done to annual glacier-wide MB values in Bolibar et al. (2020), as it only gives information about the bias of a sub-period of the reconstructions instead of the accuracy found via cross-validation. Our MB reconstructions are compared against ASTER geodetic MB from Davaze et al. (2020) for the 2000-2015 and 2003-2012 periods (Fig. 2 and S2) and against Pléiades geodetic MB from Berthier et al. (2014) for the 2003-2012 period (Fig. S2).

For certain glaciers, the ASTER and Pléiades geodetic MB give a less negative MB than the glaciological SMB used to train the deep learning SMB model. This fact might explain the slightly more negative trend of our reconstructions seen for the 2000-2015 and 2003-2012 periods, which experienced very negative MB after the well known summer 2003 heatwave. This is quite surprising, since both the GLACIOCLIM glaciological MB measurements and the annual glacier-wide MB data from Rabatel et al. (2016) have been calibrated with geodetic MB from photogrammetric DEMs, which have a very high spatial resolution. For some regions (i.e. Grandes Rousses), the independent geodetic MB are well within the uncertainty range of our model. However, large and steep glaciers in the Mont-Blanc massif and some other regions, such as Bossons, Talèfre and Tour display important differences. These glaciers have very large and high altitude accumulation areas, not seen in almost

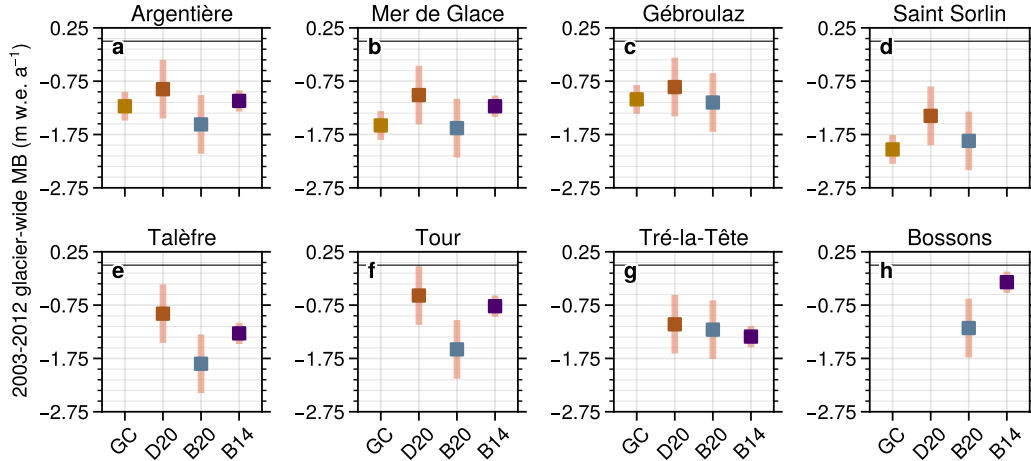


**Figure S2.** Comparison between glaciological observations from the GLACIOCLIM observatory (GC), ASTER geodetic mass balances from Davaze et al. (2020) (D20), the deep learning reconstructions from the present study (B20) and Pléiades geodetic mass balances from Berthier et al. (2014) (B14).

any glacier in our training dataset. On the other hand, several small glaciers present very important differences, with ASTER-derived MB being much less negative than our reconstructions. Data for small glaciers carry very large uncertainties, often of the same order of magnitude as the observations themselves. On top of that, flat or dome-type glaciers with large white areas with high reflectance present an important amount of noise, further increasing the associated uncertainty. This means that it is quite hard to jump to conclusions from a direct comparison between these glaciers and our reconstructions. The differences and influence of geodetic MB on the calibration of MB series should be properly studied, as they are often not taken into account as an additional uncertainty source. This topic goes beyond the scope of this study, but glacier modelling studies could benefit from integrating this in the list of uncertainties.

## 2 Model differences between the updated version of Marzeion et al. (2015) and this study

In order to contrast the results from Sect. 3.4, three important different aspects between our approach and the one of  $M_{15U}$  need to be highlighted:

1.  $M_{15U}$ 's model works with simplified physics, with a temperature-index model calibrated on observations; in this study we used a fully statistical approach based on deep learning, where physics-based considerations only appear in the predictor selection.
2.  $M_{15U}$  calibrated their model with global MB observations, including 38 glaciers in the European Alps, most of them located in Switzerland for the 1901-2013 period; in this study we used observations of 32 glaciers, all located in the French Alps for the 1967-2015 period.
3.  $M_{15U}$  forced their updated model with CRU 6.0 (update of Harris et al., 2014), with  $0.5^\circ$  latitude/longitude grid cells, which has a significantly lower spatial resolution and suitability to mountain areas than the SAFRAN reanalysis (Durand

et al., 2009) used in this study, in which altitude bands and aspects are considered for each massif, and meteorological observations from high-altitude stations are assimilated.

The cross-validations of both studies determined a performance with an average RMSE of 0.66 m.w.e.  $a^{-1}$  and an  $r^2$  of 0.43 for  $M_{15U}$  for the European Alps, and an average RMSE of 0.49 m.w.e.  $a^{-1}$  and an  $r^2$  of 0.79 for this study. However, due to the highly different methodologies and forcings of the two models, a direct comparison is not possible, so the following analysis is focused on the overall trends and sensitivities in the reconstructions and their potential sources.

### 3 Influence of area in glacier-wide MB signal and proof on non overfitting

Due to similarities between the averaged reconstructed glacier-wide MB and the observations during the 1984-2015 period, we decided to include an analysis to isolate the topographical influence in the glacier-wide MB signal, in order to verify that the model is not overfitting. Since the climate signal is the main common driver of annual variability of glacier-wide MB in the region, one needs to find a way to isolate the topographical signal. In Fig. S3, the median reconstructed annual glacier-wide MB of the 661 glaciers in the French Alps (i.e. the annual variability, hence a proxy of the climate signal) is subtracted to the mean annual values of the observations and of 4 subsets of glaciers divided by area classes. Therefore, one can observe the residual influence of glacier area on the glacier-wide MB signal. The influence of area on glaciers with observations is quite similar to glaciers with areas greater than  $2 \text{ km}^2$ , which is reasonable since glaciers with observations have an average of  $4 \text{ km}^2$  (range: 0.3-31.8  $\text{km}^2$  in 2003). Moreover, one can see that even for a relatively short period of 30 years, the differences between the reconstructions for very small glaciers ( $< 0.5 \text{ km}^2$ ) and observations are quite important, accounting for an average cumulative loss of more than 5 m.w.e. As stated in Sect. 2, this does not necessarily mean that the model has fully captured the topographical influence in the glacier-wide MB signal in the region, but it does prove that the model is not overfitting since it exhibits consistent variations in MB when the topographical predictors move away from the training data. Moreover, this is coherent with the importance attributed to topographical predictors (Bolibar et al., 2020).

The same analysis has been performed with the reconstructions from the updated version of Marzeion et al. (2015) (Fig. S4). The gradient with respect to glacier surface area appears to be similar, except for the behaviour of glaciers after 2007. Small and middle sized glaciers ( $0.1 - 2 \text{ km}^2$ ) switch to a positive influence, as opposite to large glaciers ( $> 2 \text{ km}^2$ ), which transition to a negative influence. Conversely, our results show a more continuous trend, without a change of behaviour in the last years of the analysed period.

#### 4 Supplementary figures

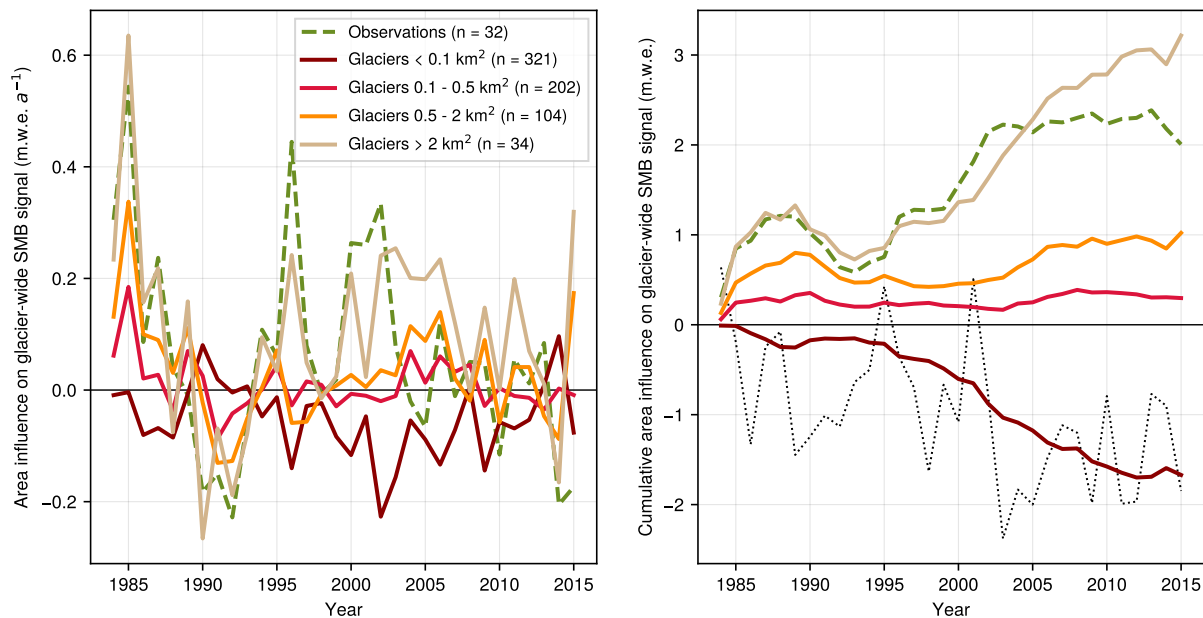


**Figure S3.** Influence of glacier area on the glacier-wide MB signal. The reconstructed median annual glacier-wide MB of the 661 glaciers in the French Alps can be seen as a proxy of the climate signal in the region. It is subtracted to the mean annual glacier-wide MB of the glaciers with observations and to four different subsets of reconstructions divided into glacier area size, showing only the annual differences based on glacier area classes. The dotted line depicts the subtracted signal (non cumulative) in order to give some context.

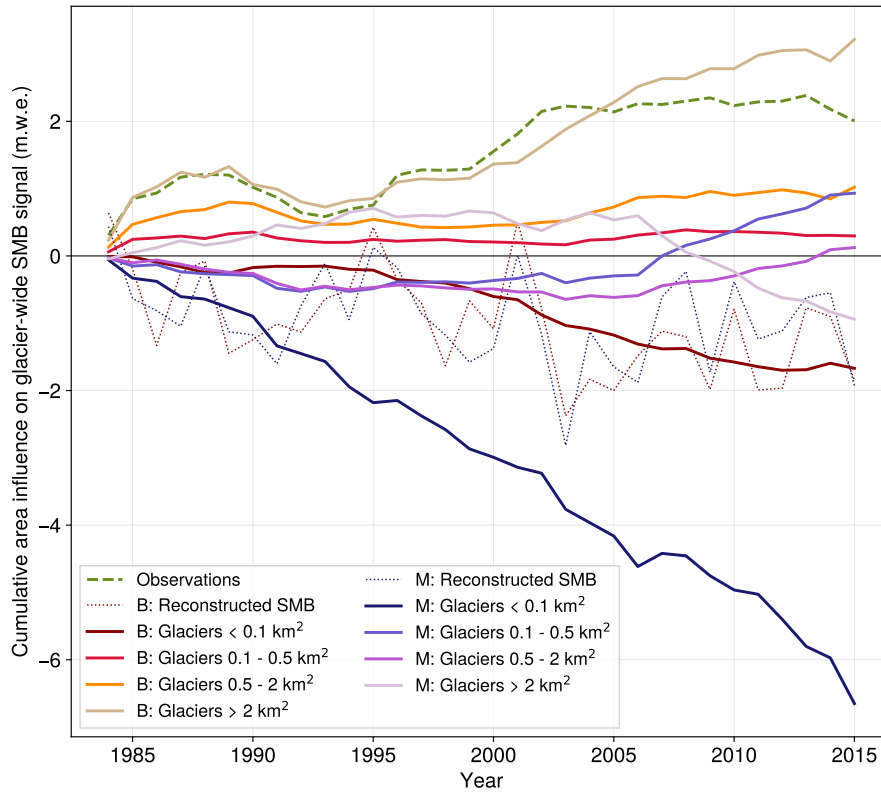


**Figure S4.** Same as S3 but comparing this study to the updated version of Marzeion et al. (2015). In the legend, “B” stands for Bolibar et al. (this study) and “M” for the update of Marzeion et al. (2015). Both models show a relatively similar gradient effect with respect to glacier area, with differences in the amplitude of the effects. The main differences appear from 2007, where small and middle sized glaciers (0.1 - 2 km<sup>2</sup>) from the update of Marzeion et al. (2015) switch to a positive influence, as opposite to large glaciers (> 2 km<sup>2</sup>), which transition to a negative influence. The reconstructed MB dotted lines are not cumulative and they are depicted in order to give some context of the subtracted climate signal.

Deep learning glacier-wide SMB simulation (1959-1983)

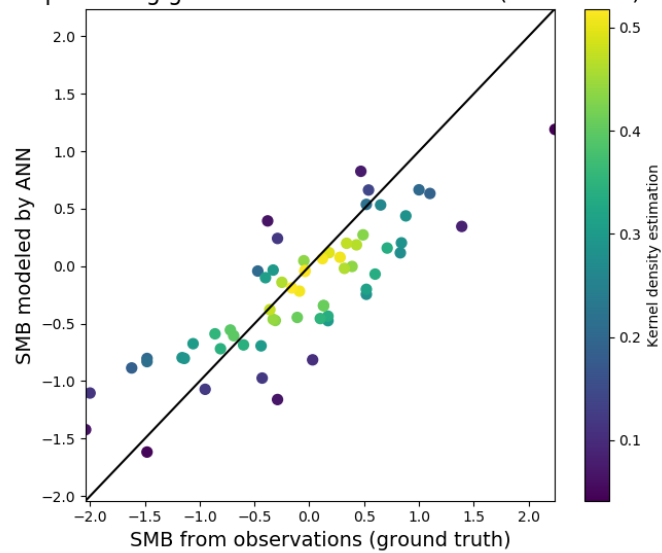


**Figure S5.** Cross-validation for annual glacier-wide MB values outside the main 1984-2014 training period. The black line indicates the one-to-one reference. Simulations have been done from 1959, the earliest date with observations to validate against the maximum number of values. This serves to confirm that the model is capable of reproducing glacier-wide MB outside the main observed period.

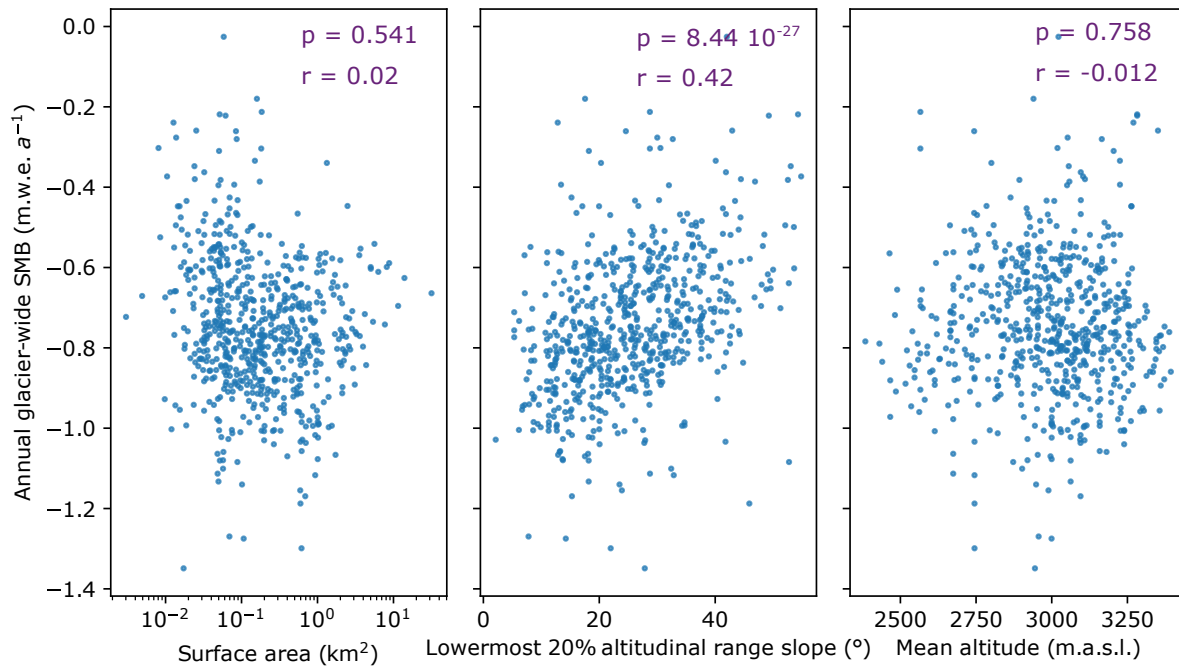


**Figure S6.** Average annual glacier-wide MB for each glacier over the entire study period with respect to (a) glacier surface area, (b) the lowermost 20% altitudinal range slope and (c) mean glacier altitude.  $p$  indicates the  $p$ -value and  $r$  the correlation between the topographical variables and the average glacier-wide MB.

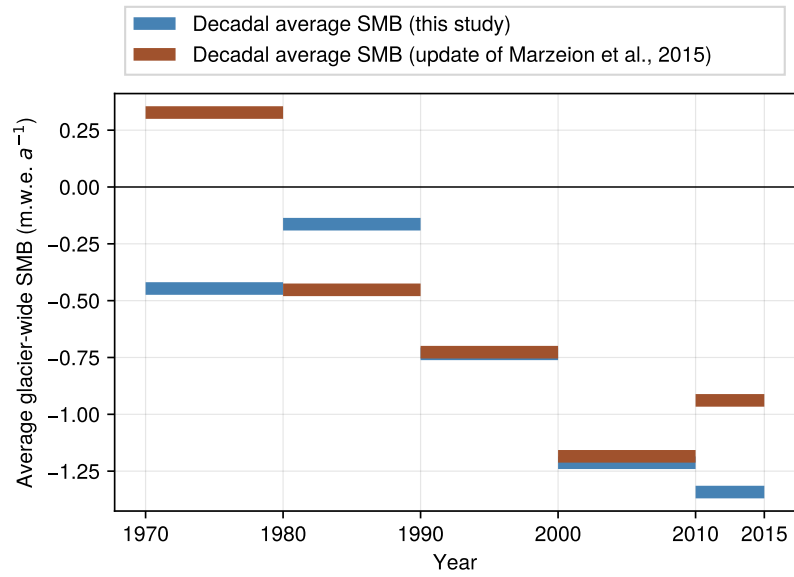


**Figure S7.** Comparison of area-weighted decadal glacier-wide MB simulations in the French Alps between this study and an update from Marzeion et al. (2015).

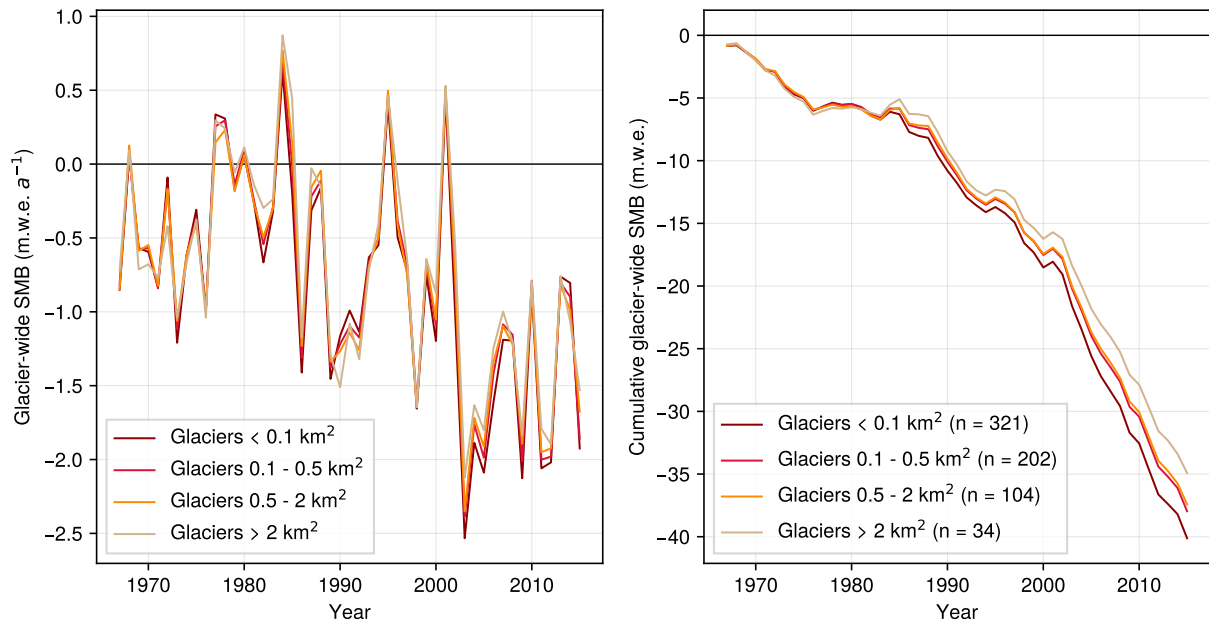


**Figure S8.** Average annual glacier-wide MB per glacier area classes

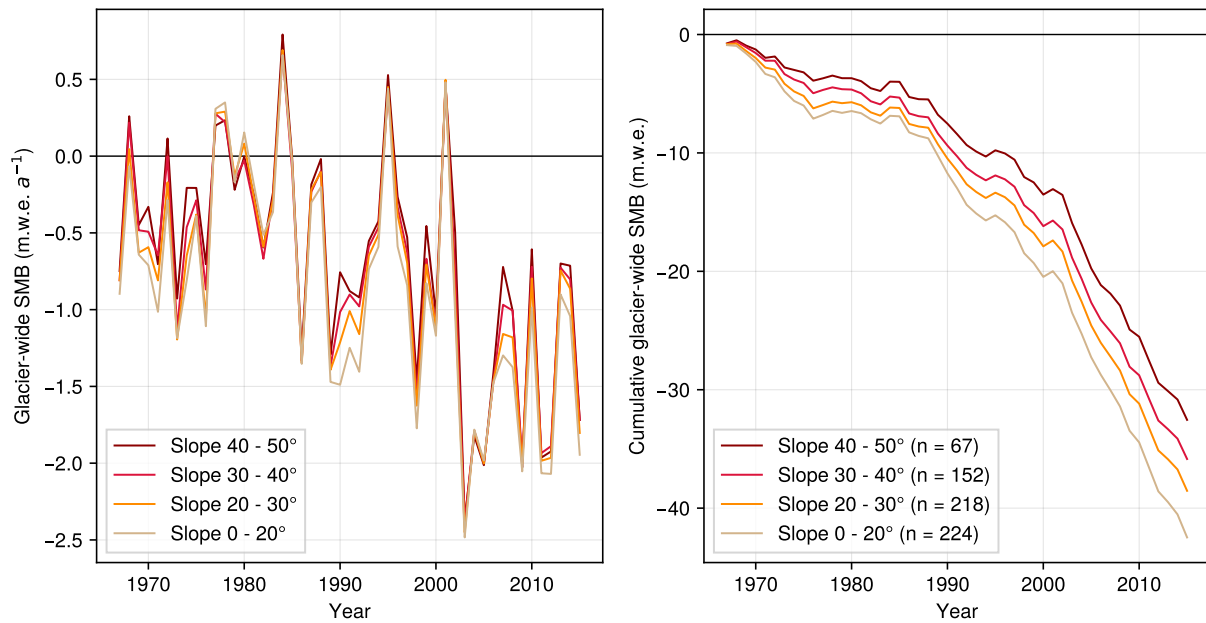


**Figure S9.** Average annual glacier-wide MB for classes of glacier slope of the lowermost 20% altitudinal range (i.e. a proxy of the glacier's tongue slope)

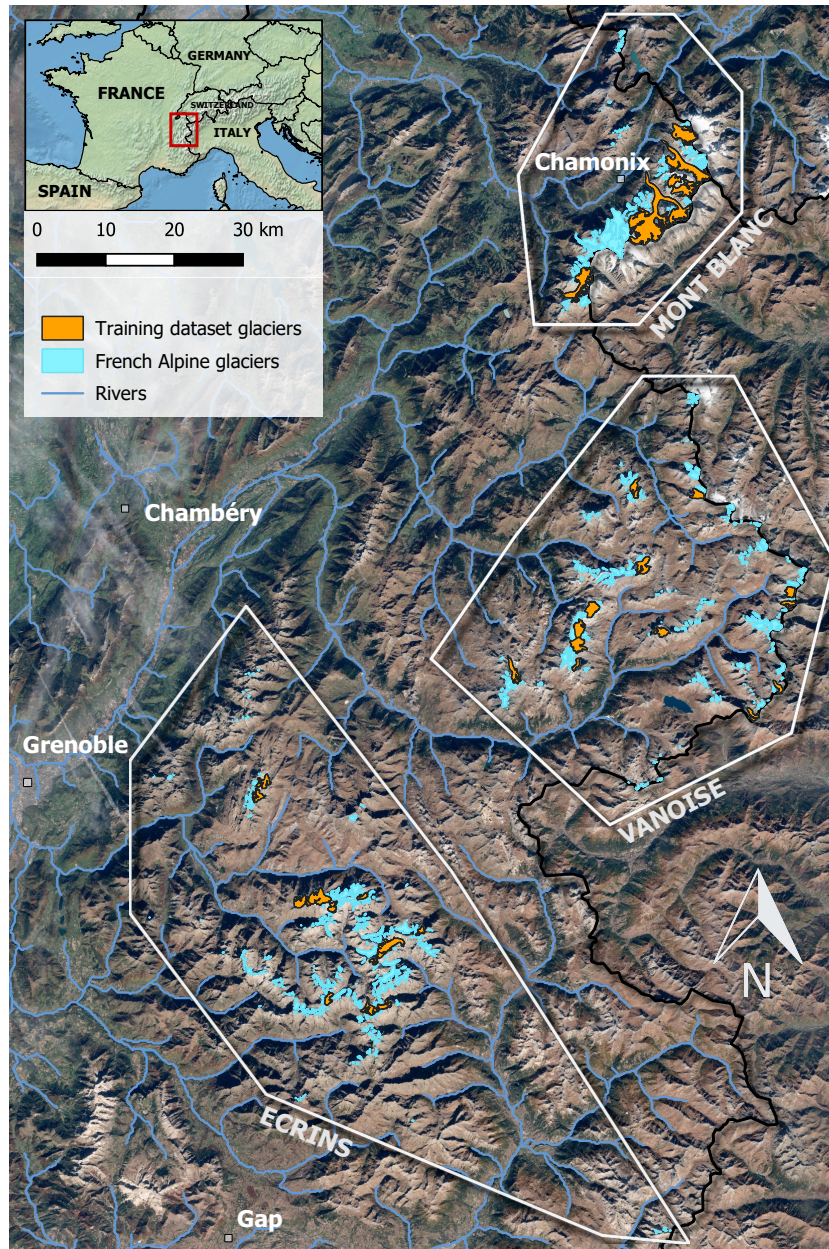


**Figure S10.** French Alpine glaciers used for model training and validation and their classification into three clusters or regions (Écrins, Vanoise, Mont-Blanc). Coordinates of bottom left map corner: 44°32' N, 5°40' E. Coordinates of the top right map corner: 46°08' N, 7°17' E.

## References

- Berthier, E., Vincent, C., Magnusson, E., Gunnlaugsson, A. T., Pitte, P., Le Meur, E., Masiokas, M., Ruiz, L., Palsson, F., Belart, J. M. C., and Wagnon, P.: Glacier topography and elevation changes derived from Pléiades sub-meter stereo images, *The Cryosphere*, 8, 2275–2291, <https://doi.org/10.5194/tc-8-2275-2014>, <https://www.the-cryosphere.net/8/2275/2014/>, 2014.
- Bolibar, J., Rabatel, A., Gouttevin, I., Galiez, C., Condom, T., and Sauquet, E.: Deep learning applied to glacier evolution modelling, *The Cryosphere*, 14, 565–584, <https://doi.org/10.5194/tc-14-565-2020>, <https://www.the-cryosphere.net/14/565/2020/>, 2020.
- Davaze, L., Rabatel, A., Dufour, A., Arnaud, Y., and Hugonnet, R.: Region-wide annual glacier surface mass balance for the European Alps from 2000 to 2016, *Frontiers in Earth Science*, 8, 149, publisher: Frontiers, 2020.
- Durand, Y., Laternser, M., Giraud, G., Etchevers, P., Lesaffre, B., and Mérindol, L.: Reanalysis of 44 Yr of Climate in the French Alps (1958–2002): Methodology, Model Validation, Climatology, and Trends for Air Temperature and Precipitation, *Journal of Applied Meteorology and Climatology*, 48, 429–449, <https://doi.org/10.1175/2008JAMC1808.1>, <http://journals.ametsoc.org/doi/abs/10.1175/2008JAMC1808.1>, 2009.
- Harris, I., Jones, P., Osborn, T., and Lister, D.: Updated high-resolution grids of monthly climatic observations - the CRU TS3.10 Dataset: UPDATED HIGH-RESOLUTION GRIDS OF MONTHLY CLIMATIC OBSERVATIONS, *International Journal of Climatology*, 34, 623–642, <https://doi.org/10.1002/joc.3711>, <http://doi.wiley.com/10.1002/joc.3711>, 2014.